



Bird, H. J.A. and Ramesh, K. (2021) Applying frequency-domain unsteady lifting-line theory to time-domain problems. *AIAA Journal*, (doi: 10.2514/1.j060898).

There may be differences between this version and the published version. You are advised to consult the publisher's version if you wish to cite from it.

<https://eprints.gla.ac.uk/261302/>

Deposited on: 12 January 2022

Enlighten – Research publications by members of the University of Glasgow
<https://eprints.gla.ac.uk>

Applying frequency-domain unsteady lifting-line theory to time-domain problems

Hugh J. A. Bird* and Kiran Ramesh†

Aerospace Sciences Division, School of Engineering, University of Glasgow, Glasgow, United Kingdom, G12 8QQ

Frequency-domain unsteady lifting-line theory is better developed than its time-domain counterpart. To take advantage of this, we propose a method to transform time-domain kinematics to the frequency domain, perform a convolution, and then return the results back to the time-domain. We demonstrate how well-developed frequency-domain methods can be easily applied to time-domain problems, enabling prediction of forces and moments on finite wings undergoing arbitrary kinematics. Results are presented for rectangular wings of various aspect ratios, undergoing pitch and heave kinematics. Computational Fluid Dynamics is used to test the effectiveness of the method in the Euler and low Reynolds number ($Re = 10000$) regimes. Overall, we find that the proposed method provides fast and reasonably accurate predictions of lift and moment coefficients, particularly in comparison to strip theory which is commonly used for problems involving arbitrary kinematics.

Nomenclature

\mathcal{R}	=	aspect ratio
c	=	chord
\bar{c}	=	mean chord
C_l	=	two-dimensional lift coefficient
C_L	=	three-dimensional lift coefficient
C_m	=	two-dimensional moment coefficient
C_M	=	three-dimensional moment coefficient
F	=	three-dimensional correction strength
g	=	return ramp function
h	=	heave displacement
h_0^*	=	non-dimensional heave oscillation amplitude
k	=	chord reduced frequency

*Graduate Researcher, h.bird.1@research.gla.ac.uk

†Senior Lecturer, Aerospace Sciences Division, School of Engineering, Kiran.Ramesh@glasgow.ac.uk, Senior Member AIAA

K	=	three-dimensional interaction kernel
P	=	ramp-hold-return amplitude
s	=	semispan
t	=	time
U_∞	=	freestream velocity
w_0, w_1, w_2	=	quadratic interpolation weights
x, y, z	=	coordinate system with origin at wing root
x_m^*	=	non-dimensional reference location for pitching moment
x_p^*	=	non-dimensional pivot location for pitching
α	=	pitch angle
α_0	=	pitch oscillation amplitude
Γ	=	bound circulation
ζ	=	spanwise coordinate
ν	=	span reduced frequency
σ	=	non-dimensional smoothing parameter for ramp-hold-return
ϕ	=	velocity potential
ω	=	angular frequency

I. Introduction

Lifting-line theory provides an elegant means by which to apply two-dimensional (2D) aerodynamic models to three-dimensional (3D) finite wing problems [1, 2]. By correcting 2D solutions for 3D effects, lifting-line theory avoids the complications of fully 3D solutions. Consequently, it can reduce computational cost and lead to a better understanding of the problem being studied.

The need for low-order methods to model the unsteady aerodynamics of finite wings in unsteady flow has led to the development of Unsteady Lifting-Line Theory (ULLT). Compared to strip theory [3], which simply sums the 2D solutions for the chord distribution along the wing, it does not neglect the often important finite-wing effects. The computational cost is far lower than fully 3D numerical methods such as the unsteady vortex lattice method [4], vortex particle methods [5–7], or computational fluid dynamics which often requires high performance computing resources. This is important in a world where unsteady aerodynamic problems involving finite wings are becoming increasingly common.

Large scale problems involve high altitude long endurance aircraft [8] and ever-larger wind turbines [9]. As scale increases, increased flexibility in the wing or turbine blade means that studying the unsteady aerodynamic response

becomes more important. More pedestrian unmanned aerial vehicles also encounter challenges due to unsteady gusts at low altitude [10, 11]. At smaller scales, a better understanding of unsteady aerodynamics eases the design of both oscillating energy harvesting devices [12] and also micro air vehicles that mimic insects using flapping wing technology.

Frequency-domain unsteady lifting-line theory is well developed. It is in effect a 3D extension of the early frequency-domain work of Theodorsen [13] and Sears [14]. Lifting-line theory is based on the assumption that the chord is much smaller than the span. When looking at the detailed flow around the wing section on the chord-scale, it is assumed to change with respect to span on the much larger span-scale. This means the problem can be modeled in 2D. When looking at the span-scale 3D problem involving the finite wing, the chord is sufficiently small that its influence can be assumed to just be on a (lifting-)line. Neither of these 2D or 3D models have enough information to model the complete 3D flow on their own. Lifting-line theory links them together to obtain a solution. The 3D model uses the bound circulation obtained from the 2D model, and the 2D model accounts for 3D effects using a correction obtained from the 3D model.

Work on frequency-domain unsteady lifting-line theory by James [15], Van Holten [16], Cheng [17], Ahmadi and Widnall [18] and Sclavounos [19] improved on the wake model by which the 2D inner problem was corrected by the simplified 3D outer problem. The importance of this wake model was demonstrated by Bird and Ramesh [20]. These models were followed by Guermond and Sellier's unsteady lifting-line theory valid for swept and curved wings oscillating at all frequencies [21].

Famously, Wagner's [22] time-domain equivalent to Theodorsen's problem [13, 23] is challenging to evaluate exactly. A consequence of this is that common approximations of Wagner's function are based on the inverse Laplace transform of Theodorsen's function [24–28]. This inverse Laplace transform depends upon the linearity of the underlying theory. For more general aerodynamic problems, time-domain results can also be obtained from the frequency domain using least-squares methods [29], which suffer from the requirement that some terms must be known *a priori*, matrix Padé methods [30], where the form of the approximation may be unstable, and combinations of the two [31]. The same property was used by Ōtomo et al. [32] to apply Theodorsen to periodic but non-sinusoidal kinematics, and in CFD to apply step responses to arbitrary kinematics [33]. Analytical time-domain methods are arguably inherently more challenging to formulate than their frequency-domain counterparts. It is therefore unsurprising that progress in time-domain unsteady lifting-line theory has been less rapid than the frequency-domain counterpart.

The earliest time domain method is that of Jones [25], where a simplified solution for an elliptic wing was obtained. More recently, Boutet and Dimitriadis [34] combined a Prandtl-like wake with Wagner's theory, and Berci obtained a method for swept wings with wake vorticity modeled using a single lumped vortex ring [35]. However, as was found by Bird and Ramesh [20], Prandtl-like wake models obtain different solutions in comparison with more complete wake models such as those used by Guermond and Sellier [21].

Numerical methods have enabled more complete wake models in the time-domain. Philips et al. [36] and Nabawy

and Crowther [37] both constructed numerical methods for flapping flight using Prandtl-like wake models. Devinant [38] constructed a numerical time-domain method based upon a simplified version of Guermond and Sellier’s frequency-domain theory [21]. This time marching theory required straight wings and uniform 3D induced downwash, in theory limiting its applicability to only low-frequency kinematics. However, Bird and Ramesh [20] found that this theoretical limitation had limited practical relevance for rectangular wing planforms. Crucially though, it modeled spanwise vorticity in the wake of the inner 2D domain and the correction for the change of the wake’s spanwise vorticity with respect to span in the outer 3D domain. This method was extended to large amplitude kinematics by Bird et al. [39] using Ramesh et al.’s [40] discrete vortex method for the 2D solutions. This 2D solution was also used by Ramesh et al. [41] in combination with a Prandtl-like wake.

In the time domain, analytical methods for finite wings are currently confined to simplified wake models. The downwash created on a wing to account for the effects of the wake of a finite wing is frequency dependent, but Prandtl-like wakes neglect this. Consequently, their accuracy is limited [20]. More complicated wake models can be constructed using numerical methods, but numerical methods typically entail increased computational costs and convergence issues. As a consequence, in practice strip theory is often used for the prediction of finite-wings undergoing unsteady motion. This paper aims to circumvent the challenge of formulating an analytical time-domain unsteady lifting-line theory by instead applying a frequency-domain ULLT to time-domain problems using Fourier transforms to perform the convolution of the input kinematics with the wing’s response in the frequency domain, taking advantage of the linearity of analytical frequency-domain ULLTs. To avoid the evaluation of the frequency-domain method at every frequency, a quadratic interpolation scheme is used. The interpolation requires only a small number of evaluations of the frequency-domain theory to obtain good results, and need only be evaluated once for a given geometry, regardless of kinematics. In comparison to matrix Padé methods and least squares approximations, the current method is simple to apply, with the complexity of the Fourier transform handled by easily available Fourier transform code libraries. In this paper, this ULLT / Convolution in Frequency Domain (UCoFD) method is applied to Sclavounos’ ULLT [19]. In theory however, the approach is independent of the details of the underlying ULLT.

This paper is laid out as follows: first, the frequency-domain ULLT used in this paper is detailed in Sec. II. This ULLT follows the work of Sclavounos with minor modifications. Next, the interpolation of frequency-domain results and the method to apply frequency-domain results to time-domain problems is introduced in Sec. III. UCoFD is then compared to CFD and strip theory for both inviscid problems and low Reynolds number problems, relevant to modern applications, in Sec. IV. Concluding remarks are made in Sec. V.

II. Frequency-domain lifting-line theory

An unsteady lifting-line theory, based on the work of Sclavounos [19], is presented in this section. Pitch and heave oscillations are considered. A more detailed derivation is given in Bird and Ramesh [20].

Sclavounos's ULLT considers a wing in inviscid, incompressible flow undergoing small-amplitude oscillation. The freestream velocity of the flow is U_∞ , and the heave h and pitch α displacement of the wing respectively are

$$h(y; t) = h_0 e^{i\omega t} = h_0^*(y) c(y) e^{i\omega t}, \quad (1)$$

$$\alpha(y; t) = \alpha_0 e^{i\omega t}, \quad (2)$$

where t is time, c is chord and ω is the angular frequency of oscillation. h_0^* is the heave oscillation amplitude h_0 non-dimensionalized by the chord, α_0 is the pitch oscillation amplitude and y is a coordinate on the span of the wing. The oscillation frequency can be non-dimensionalized by either the chord or span as

$$k(y) = \frac{\omega c(y)}{2U_\infty}, \quad (3)$$

$$\nu = \frac{\omega s}{U_\infty}, \quad (4)$$

where $k(y)$ is the local chord reduced frequency and ν is the span reduced frequency, non-dimensionalized by s , the semi-span of the wing. For the rectangular wings studied in this paper, the chord is constant with respect to span meaning $k(y)$ is constant. Consequently, it referred to as the chord reduced frequency from hereon.

Lifting-line theory assumes high aspect ratio. The inner solution is obtained on the chord scale, and can be modeled in 2D since it changes slowly with respect to span. It allows a detailed solution of flow around the chord from which quantities such as lift, moment and bound circulation can be obtained. The outer solution is obtained on the span-scale and is 3D. The chord-scale is negligible compared to the span-scale, so instead of the solving the difficult problem of 3D surface-wake interaction, the simpler problem of interaction between a (lifting-)line and the wake can be considered. These so-called inner and outer problems interact. The outer 3D problem needs detail from the inner 2D problem to obtain the bound circulation distribution, and 2D inner problem requires a correction from the outer 3D problem to account for the 3D nature of the flow. This leads to the velocity potential being taken as a 2D solution with a 3D correction given by

$$\phi(x, y, z; t) \approx \phi^{2D} + F(y)(i\omega z e^{i\omega t} - \phi_{hn}^{2D}), \quad (5)$$

where ϕ^{2D} represents the velocity potential solution to the 2D Theodorsen problem and the second term represents the correction to include 3D effects. This correction is of complex amplitude $F(y)$ and includes an oscillating uniform unit downwash velocity potential $i\omega z e^{i\omega t}$ and the reaction of the 2D airfoil section to this, ϕ_{hn}^{2D} . ϕ_{hn}^{2D} is the 2D velocity potential solution of a section oscillating in heave with unit amplitude.

When the assumptions of lifting-line theory are satisfied, this assumption of 2D flow is good. This occurs at high

aspect ratio, and for wing shapes where the chord changes slowly with respect to span. Notably, these assumptions do not hold for rectangular or elliptic wings [2]. With some formulations of unsteady lifting-line theory, these wing planforms may introduce a singularity into the results (eg. [21]), but for the current method the accuracy of the solution is merely reduced.

Theodorsen's method can be used to obtain the 2D bound circulation Γ^{2D} associated with ϕ^{2D} for both pitch and heave:

$$\Gamma_h^{2D}(y; t) = \frac{4U_\infty h_0^*(y)c(y)e^{-ik}}{iH_0^{(2)}(k) + H_1^{(2)}(k)} e^{i\omega t}, \quad (6a)$$

$$\Gamma_\alpha^{2D}(y; t) = \frac{4U_\infty \alpha_0(y)c(y)e^{-ik}}{iH_0^{(2)}(k) + H_1^{(2)}(k)} \left(\left(x_p^* - \frac{3}{4} \right) - \frac{1}{2ik} \right) e^{i(\omega t)}, \quad (6b)$$

where $H_0^{(2)}(k)$ and $H_1^{(2)}(k)$ are Hankel functions of the second kind [42] and x_p^* is the non-dimensional pivot location for pitching, where $x_p^* = 0$ indicates the leading edge and $x_p^* = 1$ indicates the trailing edge. The subscripts h and α indicate the solutions to the heave problem and the pitch problems respectively.

Following Eq. 5, this allows the corrected bound circulation to be obtained as

$$\Gamma(y; t) = \Gamma^{2D}(y; t) - F(y)\Gamma_{hn}^{2D}(t), \quad (7)$$

where subscript hn indicates the bound circulation solution for the unit heave amplitude $h_0 = 1$.

The strength of this 3D correction, $F(y)$, can be obtained from a known bound circulation distribution. For frequency-domain ULLT, Sclavounos gives this as

$$F(y) = -\frac{1}{2\pi i \omega e^{i\omega t}} \int_{-s}^s \Gamma'(\eta) K(y - \eta) d\eta, \quad (8)$$

where Γ' indicates the derivative of the bound circulation with respect to the spanwise coordinate y , and

$$K(y) = \frac{1}{2s} \operatorname{sgn}(y^*) \left[\frac{e^{-\nu|y^*|}}{|y^*|} - i\nu E_1(\nu|y^*|) + \nu P(\nu|y^*|) \right]. \quad (9)$$

$E_1(x)$ is the exponential integral [42], $y^* = y/s$ is the normalized span coordinate and

$$P(y) = \int_1^\infty e^{-yt} \left[\frac{\sqrt{t^2 - 1} - t}{t} \right] dt + i \int_0^1 e^{-yt} \left[\frac{\sqrt{1 - t^2} - 1}{t} \right] dt. \quad (10)$$

The interaction kernel $K(y)$ represents the correction for the difference between the inner 2D wake model and outer 3D wake model. In strip theory, where there is no 3D interaction, this is set to zero, giving $F_{\text{strip}} = 0$. Alternative, simplified

interaction kernels are considered in Bird et al. [20].

$F(y)$ can be substituted into Eq. 7 to obtain a differential equation that allows the inner and outer solution to be solved simultaneously:

$$\Gamma(y, t) - \frac{\Gamma_{hn}^{2D}(t)}{2\pi i \omega e^{i\omega t}} \int_{-s}^s \Gamma'(\eta) K(y - \eta) d\eta = \Gamma^{2D}(y, t), \quad (11)$$

Usually, a solution is obtained by approximating the bound circulation distribution as a truncated Fourier series

$$\Gamma(y, t) = 4U_\infty s \sum_{m=1}^M \Gamma_m \sin(m\zeta) e^{i\omega t}, \quad (12)$$

where $y = -s \cos(\zeta)$. This is solved at collocation points distributed over the span.

Theodorsen's method allows the 2D lift and moment coefficients C_l and C_m to be obtained for both pitch and heave problems

$$C_{l_h}(y; t) = 2\pi h_0^* (-2ikC(k) + k^2) e^{i\omega t}, \quad (13a)$$

$$C_{l_\alpha}(y; t) = 2\pi\alpha_0 \left[C(k) \left(1 - 2ik \left(x_p^* - \frac{3}{4} \right) \right) + \frac{ik}{2} + k^2 \left(x_p^* - \frac{1}{2} \right) \right] e^{i(\omega t + \psi)}, \quad (13b)$$

$$C_{m_h}(y; t) = 2\pi h_0^* \left[-2ikC(k) \left(x_m^* - \frac{1}{4} \right) + k^2 \left(x_m^* - \frac{1}{2} \right) \right] e^{i\omega t}, \quad (13c)$$

$$C_{m_\alpha}(y; t) = 2\pi\alpha_0 \left[C(k) \left(1 - 2ik \left(x_p^* - \frac{3}{4} \right) \right) \left(x_m^* - \frac{1}{4} \right) + k^2 \left(x_p^* \left(x_m^* - \frac{1}{2} \right) - \frac{1}{2} \left(x_m^* - \frac{9}{16} \right) \right) + \frac{ik}{2} \left(x_m^* - \frac{3}{4} \right) \right] e^{i(\omega t + \psi)}, \quad (13d)$$

where $C(k) = \frac{K_1(ik)}{K_1(ik) + K_0(ik)}$ is Theodorsen's function in terms of modified Bessel functions of the second kind [42], and x_m^* is the non-dimensional reference location about which the pitching moment is calculated.

These force coefficients can be corrected for 3D effects using Eq. 5 as

$$C_l(y; t) = C_l^{2D}(y; t) - F(y) C_{l, hn}^{2D}(y; t), \quad (14a)$$

$$C_m(y; t) = C_m^{2D}(y; t) - F(y) C_{m, hn}^{2D}(y; t). \quad (14b)$$

where $C_{l, hn}^{2D}$ and $C_{m, hn}^{2D}$ indicated the lift and moment coefficient for an airfoil oscillating in heave with amplitude $h_0 = 1$.

For a whole wing with mean chord \bar{c} , this allow lift and moment coefficients to be found as

$$C_L = \frac{1}{2s\bar{c}} \int_{-s}^s C_l(y) c(y) dy, \quad C_M = \frac{1}{2s\bar{c}^2} \int_{-s}^s C_m(y) c^2(y) dy. \quad (15)$$

III. Applying frequency-domain methods to time-domain results

For the UCoFD method to apply frequency-domain ULLT to time-domain problems, frequency domain solutions must first be obtained for the entire frequency spectrum. Evaluating the frequency-domain solution at every frequency is computationally expensive and unnecessary. Instead, the solutions can be interpolated with respect to frequency.

A lifting-line theory takes a 2D method and corrects for 3D effects. The 2D inner solution is dominant. Examining the lift and moments obtained from 2D (Eq. 13), it can be observed they are of $O(k^2)$. They can be interpolated quadratically using the weighting scheme

$$w_0(\omega) = \frac{(\omega - \omega_1)(\omega - \omega_2)}{(\omega_0 - \omega_1)(\omega_0 - \omega_2)}, \quad (16a)$$

$$w_1(\omega) = \frac{(\omega - \omega_0)(\omega - \omega_2)}{(\omega_1 - \omega_0)(\omega_1 - \omega_2)}, \quad (16b)$$

$$w_2(\omega) = \frac{(\omega - \omega_0)(\omega - \omega_1)}{(\omega_2 - \omega_0)(\omega_2 - \omega_1)}, \quad (16c)$$

which can then be applied to obtain C_L or C_M as

$$C_{L/M}(\omega) = w_0(\omega)C_{L/M}(\omega_0) + w_1(\omega)C_{L/M}(\omega_1) + w_2(\omega)C_{L/M}(\omega_2) \quad (17)$$

where $\omega_0 < \omega_1 < \omega_2$ and $\omega_0 < \omega < \omega_2$ when interpolating. Extrapolation is necessary at high frequencies.

This interpolation strategy is surprisingly effective. Figure 1 shows a 5 frequency interpolation for an aspect ratio 4 rectangular wing with the ULLT evaluated at $k = \{0.001, 0.15, 0.5, 1.2, 2.0\}$. This set of reduced frequencies is used for constructing the interpolation of all cases in this paper.

Interpolation provides excellent results even if only a small number of frequencies are evaluated for a given wing planform, even though extrapolation is required for high frequencies. For any given wing, this frequency domain result need only be obtained once.

Traditionally, time-domain schemes have combined step-function responses (indicial functions) with Duhamel integrals to obtain a response with respect to arbitrary inputs. This is a convolution of the input kinematics with the step response. To avoid the challenge of obtaining the step response, in the UCoFD method the convolution is performed in the frequency domain. This is done by taking the Fourier transform of the input kinematics, taking the convolution of this with the force response, and then taking the inverse Fourier transform. For a heave displacement $h(t)$ or pitch angle $\alpha(t)$ the following can be applied:

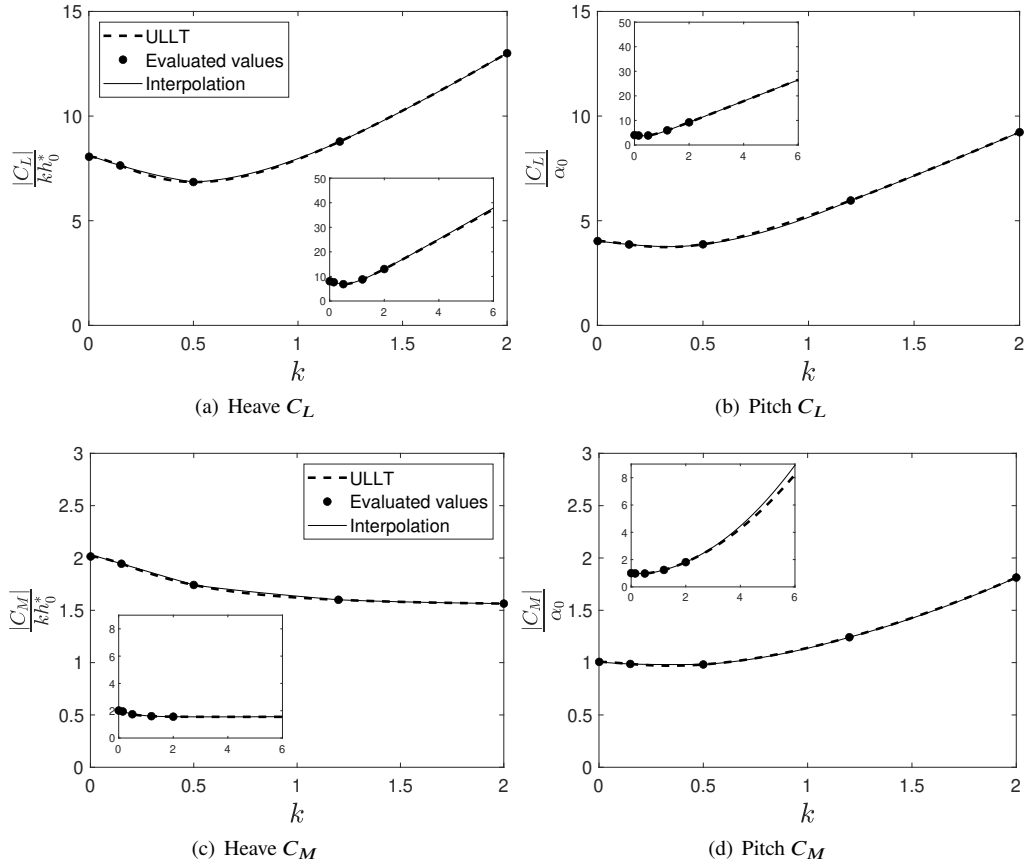


Fig. 1 Interpolation of lift and moment coefficients with respect to reduced frequency for a rectangular aspect ratio 4 wing. Moments are taken about the mid-chord. Inset shows extended frequency range result. The ULLT is evaluated at $k = \{0.001, 0.15, 0.5, 1.2, 2.0\}$ to obtain the interpolation, which is given by the solid line.

$$C_{L_h}(t) = \mathcal{F}^{-1} (\mathcal{F}(h(t)) \cdot C_{L_h}(\omega)), \quad (18)$$

$$C_{M_h}(t) = \mathcal{F}^{-1} (\mathcal{F}(h(t)) \cdot C_{M_h}(\omega)), \quad (19)$$

$$C_{L_\alpha}(t) = \mathcal{F}^{-1} (\mathcal{F}(\alpha(t)) \cdot C_{L_\alpha}(\omega)), \quad (20)$$

$$C_{M_\alpha}(t) = \mathcal{F}^{-1} (\mathcal{F}(\alpha(t)) \cdot C_{M_\alpha}(\omega)). \quad (21)$$

This can be done quickly and easily using readily available fast Fourier transform software packages. Note that for negative angular frequencies, the complex conjugate of the coefficient can be used as $C_{L/M}(-\omega) = \overline{C_{L/M}(\omega)}$.

By taking the Fourier transform of the input kinematics we assume that they are periodic. In practice if the time window passed into the Fourier transform is sufficiently large, this does not matter. The only caveat is that the displacement of the wing at the beginning and end of the time window should be the same.

IV. Results and discussion

Currently, strip-theory is often used to obtain solutions to time-domain unsteady finite wing problems quickly. In this section frequency-domain unsteady lifting-line theory is applied to time-domain problems using the UCoFD method, and the results obtained are compared against those from computational fluid dynamics and the often-used strip theory for both inviscid and low-Reynolds-number cases ($Re=10\,000$). The CFD setup is detailed in Sec. IV.A, with the Euler setup specific aspects given in Sec. IV.A.1, and the low Reynolds number specific aspects given in Sec. IV.A.2. The CFD results obtained from these setups serve as a reference against which the results obtained from the UCoFD method and strip-theory can be compared. The six cases studied are shown in Table 1.

These cases are based on the canonical ramp-hold-return kinematics of OI et al. [43]. These kinematics were chosen to demonstrate time-domain problems applicable to flapping flight where both circulatory and added-mass effects are prevalent. Case 1 (Sec. IV.B) is a leading-edge pitch ramp-hold-return in the Euler regime ($Re = \infty$), for which the UCoFD method is expected to work well. Next Case 2, in Sec. IV.C, is a Euler regime heave velocity ramp-hold-return that introduces complications with respect to having a non-zero final displacement and being less smooth. For these Euler cases, rectangular aspect-ratio 4 wings with squared off tips and a NACA0004 section are studied. This thin section is chosen to match the assumption of a thin wing section and Kutta condition at the trailing edge. Finally, in Sec. IV.D, Cases 3a-3d are leading-edge pitch ramp-hold-returns at $Re=10\,000$ (a regime representative of modern engineering problems). Pitch ramp-hold-return kinematics are applied to wings, for both small-amplitude $\alpha_{\max} = 3^\circ$ and large-amplitude $\alpha_{\max} = 25^\circ$ kinematics. These wings are rectangular, of aspect ratios 6 and 3, have squared off tips, and a NACA0008 airfoil section.

Table 1 Cases for comparison between UCoFD, CFD and strip theory.

Case	Reynolds No.	Aspect ratio	Kinematics
1	∞	4	Small-amplitude smooth pitch ramp-hold-return
2	∞	4	Small-amplitude non-smooth heave velocity ramp-hold-return
3a	10 000	6	Small-amplitude smooth pitch ramp-hold-return
3b	10 000	6	Large-amplitude smooth pitch ramp-hold-return
3c	10 000	3	Small-amplitude smooth pitch ramp-hold-return
3d	10 000	3	Large-amplitude smooth pitch ramp-hold-return

A. Computational fluid dynamics

The open-source CFD toolbox OpenFOAM was used to perform numerical computations. For both Euler and low-Reynolds-number case, a body-fitted, structured computational mesh is moved according to prescribed heave and pitch kinematics, and the time-dependent governing equations are solved using a finite volume method. A second-order backward implicit scheme is used to discretize the time derivatives, and second-order limited Gaussian integration schemes are used for the gradient, divergence and Laplacian terms. Pressure-velocity coupling is achieved using the pressure implicit with splitting of operators (PISO) algorithm. The symmetrical nature of the wing and kinematics allowed the problem to be modeled with a symmetry boundary condition at the wing root. For the far-field, freestream (inlet/outlet) boundary conditions are used. This behaves as a zero-gradient condition when fluid is flowing out of the boundary face, and as a fixed value condition (equal to freestream) when fluid is not flowing out. The wing surface uses a slip wall boundary condition for the Euler problem, and a no-slip wall for the low-Reynolds-number problem.

1. Euler cases

The Euler cases are modeled using an in-house setup that has previously been used to validate unsteady potential flow solutions for an airfoil [44] and for rectangular wings [20]. This article shares the detailed setup and meshes of the latter. The setup is intended to model the regime for which the current ULLT was derived - that is, inviscid, incompressible flow with small perturbations. Laminar flow is considered with kinematic viscosity set to zero, and a slip boundary condition is employed for the moving wing surface.

Since the kinematics are symmetric about the wing center, the cylindrical O-mesh is constructed for only half the wing. The mesh has 160 cells around the wing section, the resolution increasing near the leading and trailing edges. In the wall-normal direction, the mesh has 115 cells with the far-field extending 20 chord lengths in all directions around the section. In the spanwise direction, the mesh has 199 cells over the semispan of the wing with the resolution increasing near the wingtip. The spanwise domain extends 100 cells beyond the wingtip, to a total of 5 chord lengths.

2. Low Reynolds number cases

The $Re=10\,000$ cases were computed following the experimentally-validated RANS method used in Bird et al. [45], albeit with different kinematics. The Spalart-Allmaras (SA) turbulence model [46] is used for turbulence closure, with the trip terms in the original SA model turned off. For the low Reynolds number cases considered in this research, the effects of the turbulence model are confined to the shed vortical structures and wake.

The meshes are the same as those used in Bird et al. [45]. In this paper, two rectangular wings of chord length $c = 0.1$ m and aspect ratios 6 and 3 are considered. An O-mesh topology was used with 116 cells in the chordwise direction. The mesh was finer near the leading and trailing edges. Since the pitch kinematics are symmetrical about the wing center, only half the wing was meshed. The aspect ratio 6 and 3 half-wing meshes had 211 and 105 cells respectively in the spanwise direction. The spanwise domain extends 4 chord lengths beyond the wingtip with an average spacing of 21 cells per chord length in this region. In the wall-normal direction, cell spacing begins at 1.5×10^{-5} m next to the wall ($y+ < 1$) and extends a distance of 11.5 chord lengths away from the wing with an average density of 16.3 cells per chord length. The simulations were carried out at a free stream velocity $U_\infty = 0.1$ m/s and kinematic viscosity 10^{-6} m²/s to obtain a chord-based Reynolds number of 10 000.

B. Case 1: a returning pitch ramp in the Euler regime

A canonical pitch ramp-hold-return motion [43] is expressed as

$$\alpha(t) = \frac{P}{a\bar{c}} \left[\frac{\cosh(aU_\infty(t-t_1)/\bar{c}) \cosh(aU_\infty(t-t_4)/\bar{c})}{\cosh(aU_\infty(t-t_2)/\bar{c}) \cosh(aU_\infty(t-t_3)/\bar{c})} \right]$$

where $a = \pi^2/(4(t_2 - t_1)(1 - \sigma))$ and the wing pitches about the leading edge. This ramp-hold-return motion has the advantage that the start and end displacement is identical - unlike for the heave velocity ramp-hold-return studied in the next subsection. Here P set to give $\alpha_{\max} = 3^\circ$, and the time parameters are set to $t_1^* = 1$, $t_2^* = 3$, $t_3^* = 4$ and $t_4^* = 6$, where $t^* = tU_\infty/\bar{c}$. The smoothness of the curve is dictated by σ , which was set to 0.5 in this case. The kinematics are shown in Fig. 2. A window of $t^* = [-10, 20]$ is used here, despite the input signal of interest being in $t^* = [0, 7]$ (inset). A large window is required in comparison to that of the input signal since the Fourier transform with limited lower bounds on input frequency effectively assumes that the input is periodic. Consequently, a large window avoids the issues introduced by periodicity.

These input kinematics were evaluated at 2048 evenly spaced points in the $t^* = [-10, 20]$ window. For a problem involving a rectangular aspect ratio 4 wing of chord $c = 0.0762$ m in a freestream of $U_\infty = 0.1312$ m s⁻¹, this gives a sample interval of $\Delta t \approx 0.015$ s, resulting in a Nyquist critical frequency of $\omega_c = 2\pi/2\Delta t = 369$ rad s⁻¹ which corresponds to a critical chord reduced frequency of $k_c = 107$. This is sufficiently high to capture the highest frequency present in the input signal.

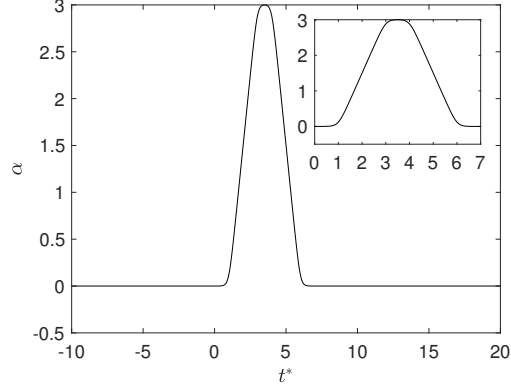


Fig. 2 Leading edge pitch ramp kinematics.

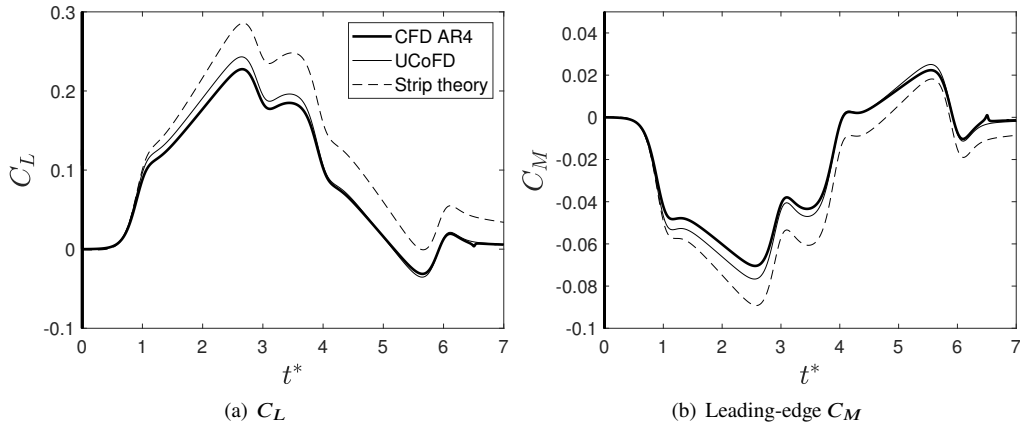


Fig. 3 Comparison of UCoFD, CFD and strip theory results for an aspect ratio 4 rectangular wing undergoing a smooth pitch ramp maneuver.

The C_L and C_M results obtained using CFD, UCoFD and strip theory are shown in Fig. 3.

The CFD results in Fig. 3(a) show the lift increasing and then returning to zero, roughly in line with the input ramp kinematics. Two mechanisms create lift. Firstly, the acceleration of the wing leading to added mass effects. The positive acceleration at $t^* = 1$ leads to a very rapid initial increase in lift. The negative acceleration either side of the peak at $t^* = 3$ and $t^* = 4$ leads to a reduction in lift. The positive acceleration at $t^* = 6$, from negative to zero rate of pitch, leads to an increase in lift. Secondly, circulatory effects lead to the overall shape of the curve, where lift is approximately proportional to the effective angle of attack [47]. The circulatory and acceleratory effects sum to the more complex final lift curve.

The shape of the C_L curve is well matched by the unsteady lifting-line theory result, although the lift peak is slightly overestimated. The error in the results is due to the application of lifting-line theory to lower aspect ratio, rectangular wings. In contrast, strip theory significantly overestimates the peak lift and introduces a slowly decaying lift that does not reflect the results obtained from the CFD.

The moment coefficients, shown in Fig. 3(b), tell a similar story. The CFD result shows the C_M to be a combination

of acceleratory effects, which lead to rapid changes in C_M , and circulatory effects, which lead to the overall shape of the curve. This is reflected well by the ULLT result, except for a small overestimation of the peak value of C_M . Again, strip theory significantly overestimates the peak value of the coefficient, and fails to return to zero as quickly as the CFD result.

For this pitch case the assumptions made in the derivation of the ULLT were satisfied (excepting the rectangular wing shape), and the fast Fourier transform could be applied without complication. This leads to good results from the UCoFD method. Next, a more challenging case will be examined, introducing two complications. Firstly, a less smooth input function will be used. This introduces higher frequency terms that may introduce errors to the result of the ULLT. And secondly, the input kinematics will not return to zero, and an artificial return ramp must be introduced.

C. Case 2: a non-returning heave velocity ramp in the Euler regime

In this subsection, the canonical ramp-hold-return motion is once again used [43], but instead of being applied to pitch angle it is applied to heave velocity. As a consequence, the net heave displacement is non-zero.

The ramp-hold-return motion is defined by the heave velocity $\dot{h} = dh/dt$ as

$$\dot{h} = \frac{P}{a} \left[\frac{\cosh(aU_\infty(t-t_1)/\bar{c}) \cosh(aU_\infty(t-t_4)/\bar{c})}{\cosh(aU_\infty(t-t_2)/\bar{c}) \cosh(aU_\infty(t-t_3)/\bar{c})} \right],$$

where $a = \pi^2/(4(t_2-t_1)(1-\sigma))$ and P set to give $\dot{h}_{\max} = -0.05\bar{c}$, and the timing parameters are $t_1^* = 1$, $t_2^* = 3$, $t_3^* = 4$ and $t_4^* = 6$. The curve smoothness parameter σ is set as 0.888, which results in less smooth motion in comparison to the pitch ramp used for Case 1 in Sec. IV.B.

The displacement at the end of the heave velocity ramp is not equal to that at the beginning. Consequently, for the UCoFD method using a window $t^* = [-10, 35]$, there is a step from $t^* = 35$ to $t^* = -10$. This must be mitigated to obtain good results.

To remove the jump, a smooth return function must be inserted. Here a quadratic return ramp is used. This ramp is given by

$$g(t) = \begin{cases} 1, & \text{if } t \leq t_{s_0} \\ 1 - 2 \left(\frac{t-t_{s_0}}{t_{s_1}-t_{s_0}} \right)^2, & \text{if } t_{s_0} < t \leq (t_{s_0} + t_{s_1})/2 \\ 2 \left(\frac{t_{s_1}-t}{t_{s_1}-t_{s_0}} \right)^2, & \text{if } (t_{s_0} + t_{s_1})/2 < t \leq t_{s_1} \\ 0, & \text{if } t > t_{s_1} \end{cases} \quad (22)$$

To obtain a displacement function which returns to zero, $h'(t)$, the original heave ramp is multiplied by the return function, giving $h'(t) = h(t)g(t)$. For a problem where the heave ramp is in $t^* = [0, 7]$ and the investigation window is in $t^* = [-10, 35]$, the return ramp used parameters $t_{s_0}^* = 10$ and $t_{s_1}^* = 20$. This places it immediately after the results of

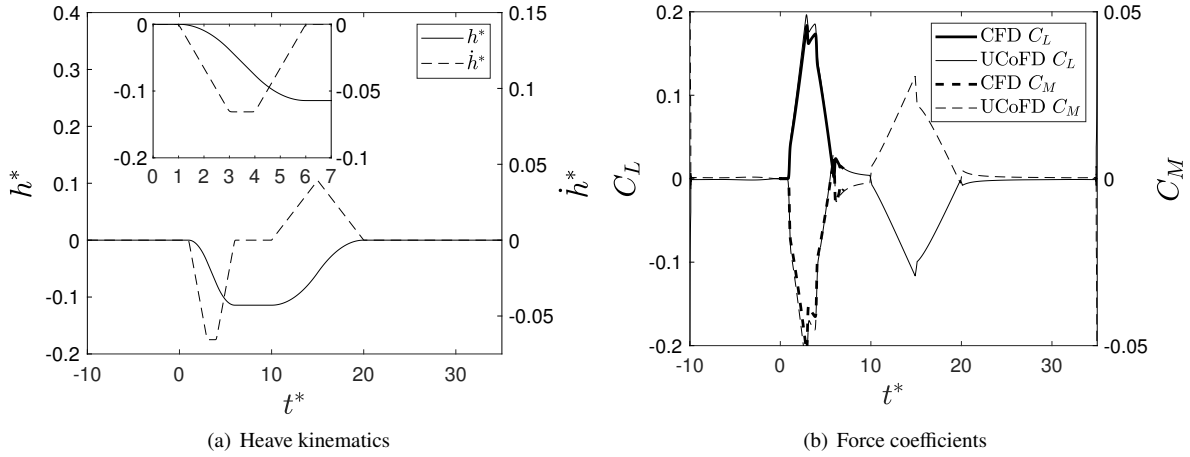


Fig. 4 Heave ramp kinematics and results for an aspect ratio 4 rectangular wing. More detailed force results are given in Fig. 5.

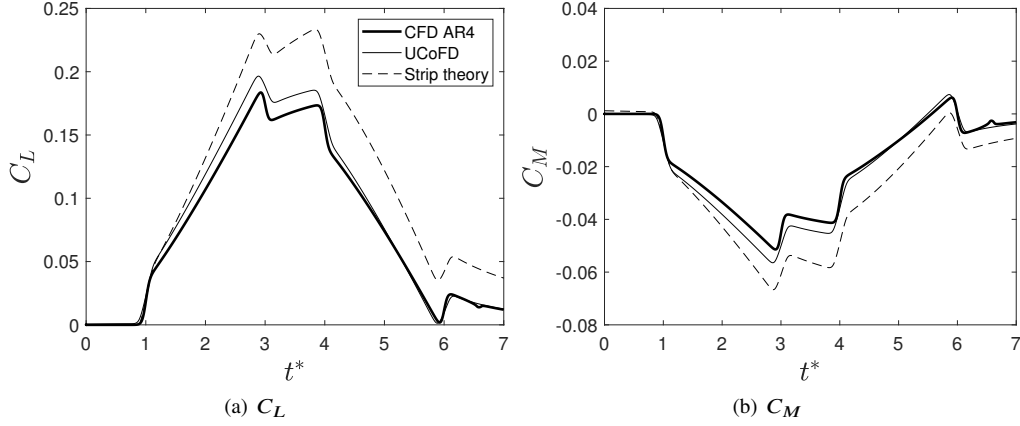


Fig. 5 Comparison of UCoFD, CFD and strip theory results for an aspect ratio 4 rectangular wing undergoing a non-smooth heave velocity ramp maneuver.

interest, allowing a large separation between the return ramp and, given the results are periodic, the beginning of the input kinematics. These kinematics are applied to the same wing used for Case 1 in Sec. IV.B, with results obtained using a 2048-sample fast Fourier transform.

The input kinematics and the results obtained for the rectangular wing are shown in Fig. 4

In Fig. 4(a), the heave ramp of interest can be seen in $t^* = [0, 7]$ (inset). This ramp results in a non-zero displacement by $t^* = 7$. As discussed earlier, a return ramp is introduced to avoid a step between $t^* = 35$ and $t^* = -10$. This ramp is separated from the kinematics of interest. The reason for this can be seen at $t^* = 20$ in Fig. 4(b), where it takes time for the forces on the wing to return to zero after the return ramp has finished.

Detailed force coefficient results in the interval of interest are shown in Fig. 5. The CFD results for both the C_L and C_M curves shows an increase in force, a plateau, and a reduction in force. The non-smoothness of the input kinematics

is reflected by the sudden change in C_L and C_M found at $t^* = \{1, 3, 4, 7\}$, where the rapid change in the acceleration of the wing leads to changes in the forces due to added-mass effects.

The ULLT / convolution in frequency domain method again predicts the CFD result with good accuracy. The overall shape of the C_L and C_M curves are well predicted, including the strength of the peaks resulting from added mass effects. This suggests that the theoretical asymptotic limitation of the underlying frequency-domain ULLT is of little practical consequence. Again, the ULLT slightly over-predicts the peak values of the forces. However, this error is small, especially when compared to the error introduced if strip-theory were to be used instead.

It has been demonstrated how a frequency-domain ULLT can be applied successfully to time-domain problems using the UCoFD method, and that it gives superior results to strip theory. However, the analytical frequency-domain ULLTs to which this technique can be applied almost universally assume potential flow and small amplitude kinematics. In the next section, the results obtained when these assumptions are broken are examined.

D. Cases 3a-3d: large amplitude pitch ramp at $Re=10\,000$

To solve for the aerodynamics in research areas such as micro air vehicles, unmanned aerial vehicles [10] or energy harvesting devices [12], solutions for low-Reynolds number, high-amplitude kinematics problems are required. The linear, potential-flow based model used in the derivation of Sclavounos' ULLT obtains surprisingly good results for frequency-domain problems in this regime [45] given that the assumptions used in its derivation are broken. Here, time-domain cases are explored using the UCoFD method.

Two rectangular wings, one of aspect ratio 6 (Cases 3a and 3b) and the other of aspect ratio 3 (Cases 3c and 3d), undergo a pitch ramp-hold-return maneuver at a Reynolds number of 10 000, with pitch occurring about the leading edge. This Reynolds number was chosen since it is representative of the low-Reynolds-number regime of the above applications.

The pitch ramp-hold-return maneuver is similar to that of Case 1 in Sec. IV.B. The wing pitches about its leading edge with P set to give both $\alpha_{\max} = 3^\circ$ (Cases 3a and 3c) and $\alpha_{\max} = 25^\circ$ (Cases 3b and 3d), and the timing parameters are set to $t_1 = 1$, $t_2 = 3$, $t_3 = 4$ and $t_4 = 6$. The smoothness of the curve is given by the parameter $\sigma = 0.5$.

The resulting lift and moment coefficients are shown in Fig. 6. The coefficients are normalized by the maximum angle of attack to allow for comparison. Both UCoFD and strip theory are linear, consequently their results are independent of the amplitude of the kinematics. The differences between the $\alpha_{\max} = 25^\circ$ and $\alpha_{\max} = 3^\circ$ CFD results are due to aerodynamic non-linearities.

The results for the aspect ratio 6 cases, shown in Fig. 6(a) and Fig. 6(b) will be considered first. The assumption made in the derivation on lifting-line theory that the aspect ratio is high is better satisfied by this $\mathcal{R}6$ wing than the $\mathcal{R}4$ wing used earlier. For the small amplitude $\alpha_{\max} = 3^\circ$, the UCoFD method predicts the shape of both the C_L and C_M curves well. However, it overestimates the peak lift and moment compared to the CFD, and by a much greater

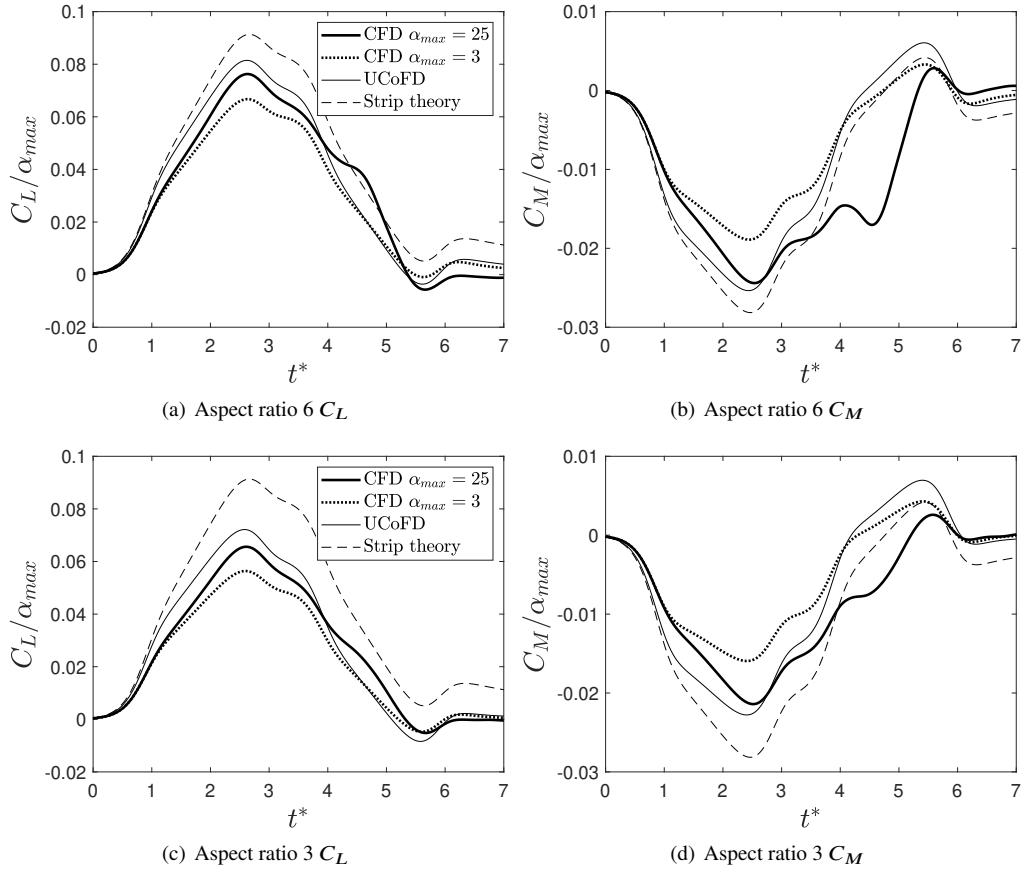


Fig. 6 Comparison of UCoFD, CFD and strip theory results for aspect ratio 6 and 3 rectangular wings undergoing a smooth pitch ramp maneuver to angles of attack of 25° and 3° at a Reynolds number of 10 000.

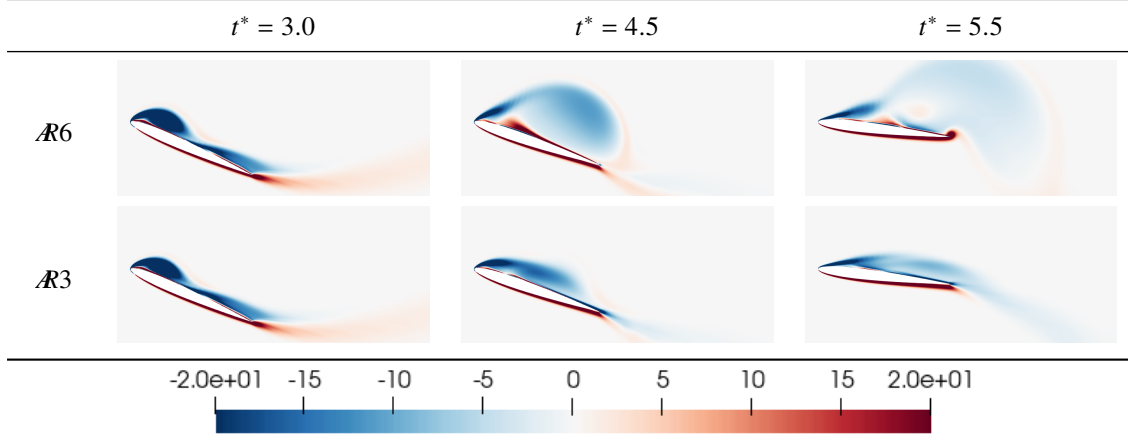


Fig. 7 Non-dimensionalized spanwise vorticity $\omega_y c/U$ at the root section of aspect ratio 6 and 3 wings, obtained from CFD at a Reynolds number of 10 000.

margin than for the Euler cases studied earlier. This is due to neglecting viscous effects which are present in the CFD at $Re = 10000$. However, the overestimation is much smaller than that produced by strip theory.

Increasing the amplitude of the kinematics from $\alpha_{\max} = 3^\circ$ to $\alpha_{\max} = 25^\circ$ has no impact on UCoFD results since the theory is linear. However, the difference in the CFD results is significant. The peak forces increase super-linearly, and the shape of the C_L and C_M curves change significantly, particularly between $t^* = 4$ and $t^* = 5$. This is due to the formation of a leading-edge vortex, that then detaches from the leading edge before being convected over the upper surface of the wing. This process is shown for both wings in Fig. 7. The UCoFD cannot model this aerodynamic non-linearity. Consequently, it is unable to reflect the change in shape of the C_L and C_M curves obtained from CFD. However, since the CFD result predicted super-linearly increasing forces, the overestimate of forces by the UCoFD has reduced. The strip theory result continues to overestimate forces more significantly than UCoFD.

At aspect ratio 3, the UCoFD over-prediction of forces in comparison to the CFD results is greater. Again, for the $\alpha_{\max} = 3^\circ$ cases, the UCoFD method correctly predicts the CFD result curve shapes. For the large amplitude $\alpha_{\max} = 25^\circ$ case, the CFD force curves are more similar to the $\alpha_{\max} = 3^\circ$ case than at aspect ratio 6. The lower aspect ratio results in a smaller and more stable leading edge-vortex (seen in Fig. 7). Consequently, the UCoFD prediction of the $\alpha_{\max} = 25^\circ$ CFD curves is better, but not excellent. In comparison, the strip theory results become worse with decreasing aspect ratio due to the increased importance of finite-wing effects.

V. Conclusions

The Unsteady Lifting-Line Theory / Convolution in Frequency Domain (UCoFD) method was derived: it allows frequency-domain unsteady lifting-line theory to be applied to time domain problems by taking the Fourier transform of the input kinematics, performing convolution with interpolated frequency-domain unsteady lifting-line results, and returning the solution to the time domain via the inverse Fourier transform.

Quadratic interpolation was used to obtain frequency domain results from several evaluations of an unsteady lifting-line theory. The Fourier transform of the time-domain kinematics, obtained using the fast Fourier transform method, is then convolved with this interpolation, before the inverse Fourier transform is applied to obtain time-domain results. Since the frequency-domain results are independent of the time-domain kinematics, they need only be computed once for a given wing geometry.

This method was compared to CFD results for a rectangular aspect ratio 4 wing in the Euler regime. Good results were obtained for both a pitch ramp case, and a heave velocity ramp case. The heave velocity ramp case also demonstrated how kinematics with different start and end points can be simulated with the current method. Compared to strip theory, the UCoFD method gave much better results.

Finally, the method was compared to a low-Reynolds number, large amplitude case. Here, the underlying assumptions used in the derivation of the method were broken, since the method doesn't model the leading edge vortex found in the CFD results. Nonetheless, UCoFD gave a reasonable prediction of lift and moment coefficients.

Acknowledgments

The authors gratefully acknowledge the support of the UK Engineering and Physical Sciences Research Council (EPSRC) through a DTA scholarship and grant EP/R008035. We also thank the Cirrus UK National Tier-2 HPC service at EPCC (<http://www.cirrus.ac.uk>) for a computing grant (Project EC114).

References

- [1] Prandtl, L., "Applications of Modern Hydrodynamics to Aeronautics," Tech. rep., NACA, 1923. Rep. 116.
- [2] Van Dyke, M., "Lifting-line theory as a singular-perturbation problem," *Journal of Applied Mathematics and Mechanics*, Vol. 28, No. 1, 1964, pp. 90–102. [https://doi.org/10.1016/0021-8928\(64\)90134-0](https://doi.org/10.1016/0021-8928(64)90134-0).
- [3] Leishman, G. J., *Principles of Helicopter Aerodynamics*, Cambridge University Press, 2006.
- [4] Simpson, R. J. S., "Unsteady Aerodynamics, Reduced-Order Modelling, and Predictive Control in Linear and Nonlinear Aeroelasticity with Arbitrary Kinematics," phdthesis, Imperial College London, 2016. URL <http://hdl.handle.net/10044/1/33327>.
- [5] Bird, H. J. A., Ramesh, K., Ōtomo, S., and Viola, I. M., "Leading Edge Vortex Formation on Finite Wings Using Vortex Particles," *AIAA Scitech 2021 Forum*, American Institute of Aeronautics and Astronautics, 2021. <https://doi.org/10.2514/6.2021-1196>.
- [6] Willis, D. J., Peraire, J., and White, J. K., "A combined pFFT-multipole tree code, unsteady panel method with vortex particle wakes," *International Journal for Numerical Methods in Fluids*, Vol. 53, No. 8, 2007, pp. 1399–1422. <https://doi.org/10.2514/6.2005-854>.
- [7] Winckelmans, G., and Leonard, A., "Contributions to Vortex Particle Methods for the Computation of Three-Dimensional

- Incompressible Unsteady Flows,” *Journal of Computational Physics*, Vol. 109, No. 2, 1993, pp. 247–273. <https://doi.org/10.1006/jcph.1993.1216>.
- [8] Shearer, C. M., and Cesnik, C. E. S., “Nonlinear Flight Dynamics of Very Flexible Aircraft,” *Journal of Aircraft*, Vol. 44, No. 5, 2007, pp. 1528–1545. <https://doi.org/10.2514/1.27606>.
- [9] Hansen, M., Sørensen, J., Voutsinas, S., Sørensen, N., and Madsen, H., “State of the art in wind turbine aerodynamics and aeroelasticity,” *Progress in Aerospace Sciences*, Vol. 42, No. 4, 2006, pp. 285–330. <https://doi.org/10.1016/j.paerosci.2006.10.002>.
- [10] Williams, W., and Harris, M., “The challenges of flight-testing unmanned air vehicles,” *Systems Engineering, Test & Evaluation Conference, Sydney Australia, 2002*.
- [11] Jones, A. R., and Cetiner, O., “Overview of NATO AVT-282: Unsteady Aerodynamic Response of Rigid Wings in Gust Encounters,” *AIAA Scitech 2020 Forum*, American Institute of Aeronautics and Astronautics, 2020. <https://doi.org/10.2514/6.2020-0078>.
- [12] Rostami, A. B., and Armandei, M., “Renewable energy harvesting by vortex-induced motions: Review and benchmarking of technologies,” *Renewable and Sustainable Energy Reviews*, Vol. 70, 2017, pp. 193–214. <https://doi.org/10.1016/j.rser.2016.11.202>.
- [13] Theodorsen, T., “General Theory of Aerodynamic instability and the mechanism of flutter,” Tech. Rep. 496, NACA, 1935.
- [14] Sears, W. R., “Some Aspects of Non-Stationary Airfoil Theory and Its Practical Application,” *Journal of the Aeronautical Sciences*, Vol. 8, No. 3, 1941, pp. 104–108. <https://doi.org/10.2514/8.10655>.
- [15] James, E. C., “Lifting-line theory for an unsteady wing as a singular perturbation problem,” *Journal of Fluid Mechanics*, Vol. 70, No. 04, 1975, p. 753. <https://doi.org/10.1017/s0022112075002339>.
- [16] Holten, T. V., “Some notes on unsteady lifting-line theory,” *Journal of Fluid Mechanics*, Vol. 77, No. 03, 1976, p. 561. <https://doi.org/10.1017/s0022112076002255>.
- [17] Cheng, H. K., “On Lifting-Line Theory in Unsteady Aerodynamics,” Tech. rep., University of Southern California Los Angeles Department of Aerospace Engineering, 1976. URL <http://www.dtic.mil/docs/citations/ADA021449>.
- [18] Ahmadi, A. R., and Widnall, S. E., “Unsteady lifting-line theory as a singular perturbation problem,” *Journal of Fluid Mechanics*, Vol. 153, 1985, p. 59. <https://doi.org/10.1017/s0022112085001148>.
- [19] Sclavounos, P. D., “An unsteady lifting-line theory,” *Journal of Engineering Mathematics*, Vol. 21, No. 3, 1987, pp. 201–226. <https://doi.org/10.1007/bf00127464>.
- [20] Bird, H. J. A., and Ramesh, K., “Unsteady lifting-line theory and the influence of wake vorticity on aerodynamic loads,” *Theoretical and Computational Fluid Dynamics*, 2021. <https://doi.org/10.1007/s00162-021-00578-8>.

- [21] Guermond, J.-L., and Sellier, A., “A unified unsteady lifting-line theory,” *Journal of Fluid Mechanics*, Vol. 229, 1991, p. 427. <https://doi.org/10.1017/s0022112091003099>.
- [22] Wagner, H., “Über die Entstehung des dynamischen Auftriebes von Tragflügeln,” *ZAMM - Zeitschrift für Angewandte Mathematik und Mechanik*, Vol. 5, No. 1, 1925, pp. 17–35. <https://doi.org/10.1002/zamm.19250050103>.
- [23] Garrick, I. E., “On some reciprocal relations in the theory of nonstationary flows,” Tech. rep., NACA, 1938.
- [24] Fung, Y. C., *An Introduction to the Theory of Aeroelasticity*, Dover Publications, 1993.
- [25] Jones, R. T., “The unsteady lift of a wing of finite aspect ratio,” Tech. rep., National Advisory Committee for Aeronautics, 1940.
- [26] Jones, W. P., “Aerodynamic forces on wings in non-uniform motion,” Tech. rep., Aeronautical Research Council, 1945.
- [27] Dowell, E., “A simple method for converting frequency-domain aerodynamics to the time domain,” Tech. Rep. NASA TM-81844, National Aeronautics and Space Administration, 1980. URL <https://ntrs.nasa.gov/citations/19800024850>.
- [28] Dawson, S. T. M., and Brunton, S. L., “Improved approximations to the Wagner function using sparse identification of nonlinear dynamics,” 2021. URL <https://www.researchgate.net/publication/351278676>, preprint.
- [29] Roger, K. L., “Airplane Math Modeling Methods for Active Control Design,” *AGARD Structures and Materials Panel*, 1977.
- [30] Vepa, R., “On the use of Pade approximants to represent unsteady aerodynamic loads for arbitrarily small motions of wings,” *14th Aerospace Sciences Meeting*, American Institute of Aeronautics and Astronautics, 1976. <https://doi.org/10.2514/6.1976-17>.
- [31] Dunn, H., “An Analytical Technique for Approximating Unsteady Aerodynamics in the Time Domain,” Tech. rep., National Aeronautics and Space Administration, 1980. URL <https://ntrs.nasa.gov/citations/19810002914>, nASA Technical Paper 1738.
- [32] Ōtomo, S., Henne, S., Mulleners, K., Ramesh, K., and Viola, I. M., “Unsteady lift on a high-amplitude pitching aerofoil,” *Experiments in Fluids*, Vol. 62, No. 1, 2020. <https://doi.org/10.1007/s00348-020-03095-2>.
- [33] Silva, W. A., “Discrete-time linear and nonlinear aerodynamic impulse responses for efficient CFD analyses,” Ph.D. thesis, College of William & Mary, 1997. URL <https://scholarworks.wm.edu/cgi/viewcontent.cgi?article=3482&context=etd>.
- [34] Boutet, J., and Dimitriadis, G., “Unsteady Lifting Line Theory Using the Wagner Function for the Aerodynamic and Aeroelastic Modeling of 3D Wings,” *Aerospace*, Vol. 5, No. 3, 2018, p. 92. <https://doi.org/10.3390/aerospace5030092>.
- [35] Berci, M., “Downwash corrections for unsteady subsonic lift,” *INTERNATIONAL CONFERENCE OF COMPUTATIONAL METHODS IN SCIENCES AND ENGINEERING ICCMSE 2020*, AIP Publishing, 2021. <https://doi.org/10.1063/5.0048585>.
- [36] Phlips, P. J., East, R. A., and Pratt, N. H., “An unsteady lifting line theory of flapping wings with application to the forward flight of birds,” *Journal of Fluid Mechanics*, Vol. 112, No. -1, 1981, p. 97. <https://doi.org/10.1017/s0022112081000311>.
- [37] Nabawy, M. R. A., and Crowthe, W. J., “A Quasi-Steady Lifting Line Theory for Insect-Like Hovering Flight,” *PLOS ONE*, Vol. 10, No. 8, 2015, p. e0134972. <https://doi.org/10.1371/journal.pone.0134972>.

- [38] Devinant, P., “An approach for unsteady lifting-line time-marching numerical computation,” *International Journal for Numerical Methods in Fluids*, Vol. 26, No. 2, 1998, pp. 177–197. [https://doi.org/10.1002/\(sici\)1097-0363\(19980130\)26:2<177::aid-flid633>3.3.co;2-g](https://doi.org/10.1002/(sici)1097-0363(19980130)26:2<177::aid-flid633>3.3.co;2-g).
- [39] Bird, H. J. A., Otomo, S., Ramesh, K., and Viola, I. M., “A Geometrically Non-Linear Time-Domain Unsteady Lifting-Line Theory,” *AIAA Scitech 2019 Forum*, American Institute of Aeronautics and Astronautics, 2019. <https://doi.org/10.2514/6.2019-1377>.
- [40] Ramesh, K., Gopalathnam, A., Edwards, J. R., Ol, M. V., and Granlund, K., “An unsteady airfoil theory applied to pitching motions validated against experiment and computation,” *Theoretical and Computational Fluid Dynamics*, Vol. 27, No. 6, 2013, pp. 843–864. <https://doi.org/10.1007/s00162-012-0292-8>.
- [41] Ramesh, K., Monteiro, T. P., Silvestre, F. J., Bernardo, A., Neto, G., de Souza Siqueria Versiani, T., and da Silva, R. G. A., “Experimental and Numerical Investigation of Post-Flutter Limit Cycle Oscillations on a Cantilevered Flat Plate,” *International Forum on Aeroelasticity and Structural Dynamics 2017*, 2017. URL <http://eprints.gla.ac.uk/154722/>.
- [42] Olver, F. W., Lozier, D. W., Boisvert, R. F., and Clark, C. W., *NIST Handbook of Mathematical Functions Paperback and CD-ROM*, Cambridge University Press, 2010.
- [43] Ol, M., Altman, A., Eldredge, J., Garmann, D., and Lian, Y., “Résumé of the AIAA FDTC Low Reynolds Number Discussion Group's Canonical Cases,” *48th AIAA Aerospace Sciences Meeting Including the New Horizons Forum and Aerospace Exposition*, American Institute of Aeronautics and Astronautics, 2010. <https://doi.org/10.2514/6.2010-1085>, AIAA 2010-1085.
- [44] Ramesh, K., “On the Leading-Edge Suction and Stagnation Point Location in Unsteady Flows Past Thin Aerofoils,” *Journal of Fluid Mechanics*, Vol. 886, No. A13, 2020.
- [45] Bird, H. J. A., Ramesh, K., Otomo, S., and Viola, I. M., “Usefulness of inviscid linear unsteady lifting-line theory for viscous large-amplitude problems,” *AIAA Journal*, 2021. <https://doi.org/10.2514/1.J060808>.
- [46] Spalart, P., and Allmaras, S., “A one-equation turbulence model for aerodynamic flows,” *30th Aerospace Sciences Meeting and Exhibit*, American Institute of Aeronautics and Astronautics, 1992. <https://doi.org/10.2514/6.1992-439>, AIAA Paper 1992-0439.
- [47] Ramesh, K., “On the leading-edge suction and stagnation-point location in unsteady flows past thin aerofoils,” *Journal of Fluid Mechanics*, Vol. 886, 2020. <https://doi.org/10.1017/jfm.2019.1070>.